

their relative positions must be determined by monitoring changes in the phases of the differential interferometric observables over a sizable fraction of a day. Lunar libration causes these apparent positions to vary over the course of a month, and longer. The differential nature of the observable sharply reduces the effects of errors in the lunar ephemeris, tracking station coordinates, and so forth, and should yield at least an order of magnitude improvement in our knowledge of the libration [present uncertainty about 10 seconds of selenocentric arc (6)].

Differential interferometric tracking of planetary probes, landers, and orbiters will yield results in many cases more accurate than can be obtained from tracking satellites of the earth. This seemingly paradoxical conclusion follows because the usual limitation is set not by signal strength but by systematic effects of the atmosphere and ionosphere, and sometimes by receiving-system phase instabilities. These effects cancel in the differential interferometric observable. A planetary application of differential interferometry which is analogous to, but more complicated than, the Lunar Rover-Lunar Module situation involves tracking a number of small probes descending simultaneously into Venus's atmosphere (7). By differential tracking of the free-falling probes relative to a parent spacecraft it should be possible to detect horizontal winds at the level of a few meters per second. Differential interferometry could also aid in the interpretation of occultation data (8). Additional applications of differential interferometry to both orbiters and landers are too numerous to be elaborated here; for example, improved estimates of the planet's gravity model parameters, rotation vector, and landing site or orbit parameters may be expected [see, for example, (8)]. Whenever the planet passes close to the direction of an extragalactic radio source, differential interferometry may be used to determine the earth-planet direction relative to that of the source to about 0.001 arc second. Such measurements could be used to determine precisely the orientation of planetary orbits with respect to an inertial frame and, for example, to monitor the perihelion precessions to further test general relativity. For ground-based radiometric mapping of the terrestrial planets, differential interferometry can overcome the effects of instrumental, atmospheric, and ionospheric phase drifts, which limit the application of aperture-synthesis tech-

niques. A phase reference could be provided, for example, by the specular echo of a radar signal sent at the appropriate frequency (9). Such mapping appears especially important for Mars where the distribution of small amounts of surface water (or ice) might be discernible from millimeter-wavelength observations (10).

In summary, the technique of differential interferometry seems capable of solving a wide range of astronomical problems.

C. C. COUNSELMAN, III
H. F. HINTEREGGER
I. I. SHAPIRO

Department of Earth and Planetary Sciences, Massachusetts Institute of Technology, Cambridge 02139

References and Notes

1. This principle has already been applied in lunar and planetary radar experiments, in mapping the relative positions of closely spaced sources in the sky, and in the detection of the differential gravitational deflection of radio signals by the sun. Our discussion concerns new applications, especially ones in which a carrier signal is available from each source.
2. A matched-filter receiver could then be used to estimate the delay at each site, in the same way as for two-way ranging. See, for example, J. V. Evans and T. Hagfors, Eds., *Radar Astronomy* (McGraw-Hill, New York, 1968), pp. 500-509. The value obtained at one site would not, by itself, be significant, but the difference between sites would. Phase delay could be measured simultaneously with group delay if a Doppler counter were also available at each site. In addition to not requiring direct recording of the signals for VLBI, artificial sources have an enormous signal-to-noise advantage over natural sources because they are coherent.
3. These stations (in Madrid, Spain; on Ascension Island; and at Cape Kennedy, Florida) belong to the Spacecraft Tracking Data Network (STDN) of the National Aeronautics and Space Administration (NASA), and are managed by Goddard Space Flight Center.
4. A detailed discussion of the algorithms used is presented by us in "The STDN Metric Tracking Performance Apollo 16 Final Report," No. X832-72-203, available from the Librarian, Goddard Space Flight Center, Greenbelt, Maryland 20771.
5. ALSEP is an acronym for Apollo Lunar Surface Experiments Package.
6. Observations of the ALSEP's to determine the lunar libration are now being considered by the STDN (3) (I. Salzberg, personal communication).
7. Space Science Board, *Venus, Strategy for Exploration* (National Academy of Sciences, Washington, D.C., 1970), pp. 33-34.
8. W. H. Michael, Jr., D. L. Cain, G. Fjeldbo, G. S. Levy, J. G. Davies, M. D. Grossi, I. I. Shapiro, G. L. Tyler, *Icarus* **16**, 57 (1972).
9. This application of differential interferometry is similar to the phase-calibration technique used for unambiguous radar delay-Doppler mapping of Venus by A. E. E. Rogers and R. P. Ingalls [*Science* **165**, 797 (1969)].
10. C. Sagan and J. Veverka, *Icarus* **14**, 222 (1971).
11. The Lunar Rover tracking results shown here resulted in part from the programming and related aid performed at Goddard Space Flight Center by E. S. Shaffer and D. Shnidman of the Bendix Company. Invaluable support was also provided by the Metric Data Branch at Goddard, and especially by the Tracking Data Evaluation Section. The Lunar Rover tracking project was headed by I. Salzberg.

19 June 1972

A Scanning X-Ray Microscope Using Synchrotron Radiation

Abstract. *Focused synchrotron radiation collimated by means of a pinhole has been used to construct a scanning x-ray microscope capable of making stereoscopic element-discriminating pictures of relatively thick specimens in an atmospheric environment.*

We have constructed an element-discriminating microscope with the soft x-ray portion of the synchrotron radiation from the Cambridge Electron Accelerator (CEA) as a source. In this report we describe the prototype design and present some results obtained during the initial weeks of operation. It is our hope that some of the microscope's unique characteristics might be useful in a variety of disciplines, and we encourage those interested in possible applications of the microscope to communicate with us.

The CEA, which is currently being used in electron-positron colliding beam experiments, is a source of synchrotron radiation. The radiation emitted by relativistic electrons of energy γmc^2 (where m is the rest mass, c is the speed of light, and γ is the "Lorentz factor" E_{total}/mc^2) moving in a circle of radius R , observed outside the orbit and in

the orbital plane, consists of a series of short electromagnetic pulses spaced apart by the orbital period $2\pi R/c$. The radiation is confined to a fan-shaped beam within an angle of order $\theta \approx 1/\gamma$ of the orbital plane, and has a spectrum (power per unit energy interval at a photon energy E) which is essentially a continuum proportional to $E^{1/2}$ up to a peak photon energy $E_p \approx \gamma^3 \mathcal{H}/R$ (where \mathcal{H} is Planck's constant), and dropping rapidly at higher energies (1).

With the CEA operating at 3 Gev, the synchrotron radiation spectrum has its peak at about 2 keV and emits copiously in the spectral region from 100 eV to 5 keV, where elements of low to moderate atomic number have their K absorption edges. Furthermore, the x-ray power emitted per unit solid angle in this part of the spectrum exceeds by three to six orders of magnitude that available from conventional x-ray tubes,

thus making possible the form of x-ray microscope to be described here. At a beam current of 15 ma, for instance, roughly 10^{14} photons per second are radiated per milliradian of orbit in a 10 percent energy band in the energy range from 100 ev to 5 kev.

The synchrotron radiation from approximately 10 milliradians of orbit is brought out through vacuum plumbing and reflected from a quartz ellipsoidal condensing mirror. Because bulk materials have a wavelength-dependent index of refraction less than unity at x-ray wavelengths, one can make an optical system with total external reflection (2). For a given wavelength, total external reflection occurs at glancing angles less than some critical angle; or, at a given glancing angle, all radiation up to some critical energy is totally reflected. Our mirror is inclined at 10 milliradians to the orbital plane, giving nearly total reflection up to an energy of 3.5 kev, and very little above that. It thus provides a high-energy cutoff, eliminating hard x-rays and high-energy bremsstrahlung from residual gas in the accelerator. Because of the mirror's ellipsoidal shape, the intensity of the transmitted radiation also increases by approximately three orders of magnitude. The mirror (3) intercepts the radiation originating from 10 milliradians of electron beam orbit, focusing it down to a spot roughly 1 by 2 mm. The focused beam of x-rays is so intense that a blue beam of air fluorescence is visible to the naked eye for about 30 cm beyond the beryllium window which terminates the vacuum beam run.

This x-ray beam, now traveling through air, is used to operate a microscope of extremely simple design. No attempt is made to form a focused x-ray image; rather, the x-ray beam is collimated to a pencil beam of micron size by passage through a pinhole formed in a heavy metal. The sample to be examined is irradiated by the emergent beam, one point at a time, while being moved in a raster pattern perpendicular to the beam axis by a mechanical transducer. Gas-filled proportional counters surrounding the beam axis detect the characteristic fluorescent x-rays emitted by the specimen and intensify the trace of a display oscilloscope whose spot is moving in synchronization with the mechanical transducer. By selecting counter pulses corresponding to the fluorescence energy of a given chemical element, one can build up a picture of the distribu-

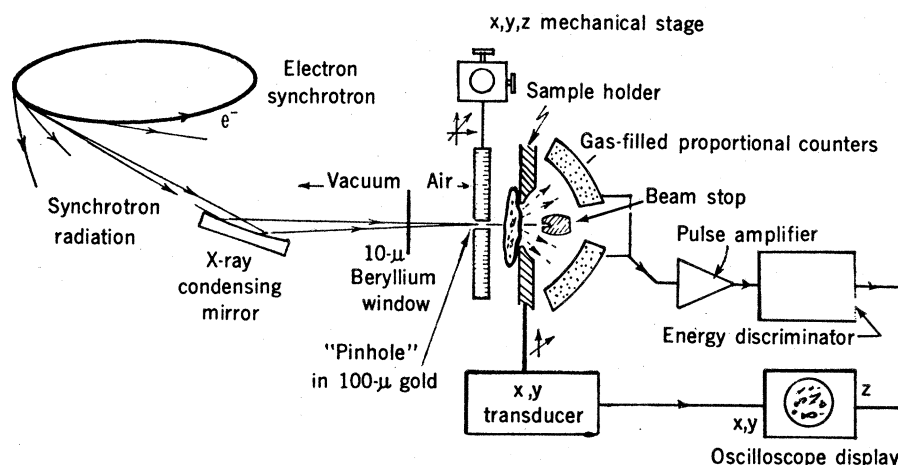


Fig. 1. Diagram of the microscope. The beam stop just behind the specimen absorbs the transmitted beam, reducing the elastically scattered background.

tion of that element across the specimen.

The important characteristics of this microscope can be discussed under the following headings:

Sample environment. At the x-ray energies involved air is reasonably transparent, and so the entire microscope is operated in an atmospheric environment. In addition to its obvious convenience, this makes possible the viewing of hydrated, or even live, specimens. Other environments could be substituted if desirable; air saturated with water vapor might be useful, for example, to prevent drying of thin specimens during exposure. Alternatively the sample could be refrigerated.

Resolution. The resolution is roughly the same as the diameter of the collimated x-ray beam, that is, the pinhole diameter, and is approximately 2μ in the present microscope. Improving the resolution involves trade-offs in both exposure time and depth of field, as will be explained below, as well as the difficulty of manufacturing submicron size pinholes. Although smaller holes can be made successfully by a variety of techniques [fission track etching (4) or the etching of directionally solidified eutectics (5)], what is needed here is a straight hole through a thickness of material sufficient to attenuate incident x-rays by many orders of magnitude. In practice, this means a submicron hole through 50 to 100μ of gold, for instance. The "pinhole" is actually a long pipe! A less dense pinhole substrate would involve even greater ratios of length to diameter and thus an undesirable reduction in the acceptance angle of incoming radiation. In our prototype microscope a $2\text{-}\mu$ hole was made by electroplating gold onto a gold substrate

from which projected a $2\text{-}\mu$ silicon whisker grown by the vapor-liquid-solid mechanism (6). This technique can probably be extended down to 0.2 to 0.5μ , but much smaller holes will require the use of some other technique.

Depth of field. The depth of field is limited either by the diffraction of the emergent x-ray beam from the pinhole aperture or by the geometry of the pinhole acceptance angle and the convergence angle of its illumination. Radiation of wavelength λ passing through a hole of diameter d will spread significantly because of diffraction after traveling a distance $L \approx d^2/\lambda$, about 8 mm for the prototype microscope. In this case, however, the depth of field is ultimately limited by the horizontal convergence of the illumination, to roughly 1000μ . This is an enormous depth of field by the standards of ordinary microscopy, a useful consequence of which is the possibility of making in-focus micrographs of the same object viewed at two angles, with subsequent stereoscopic interpretation.

Penetrating power and sample thickness. At the wavelengths of interest, 2 to 20 Å (in the vicinity of the K absorption edges of elements of moderate atomic weight), the thickness of unit density material necessary to absorb most of the incident radiation is roughly 10 to 100μ . For samples much thicker than this, very little of the incident radiation will penetrate the entire sample, and only a small fraction of the reradiated fluorescent x-rays will be able to escape from the sample and reach the detectors. For samples thinner than this upper limit, the entire thickness of the specimen is imaged by the microscope.

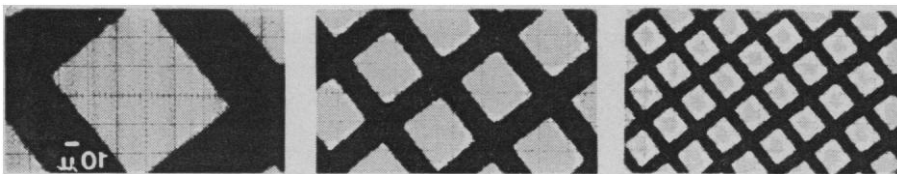


Fig. 2. Transmission micrographs of a 200 mesh per inch (80 grids per centimeter) copper grid at three different magnifications. The faint horizontal and vertical lines in these micrographs are from the oscilloscope graticule.

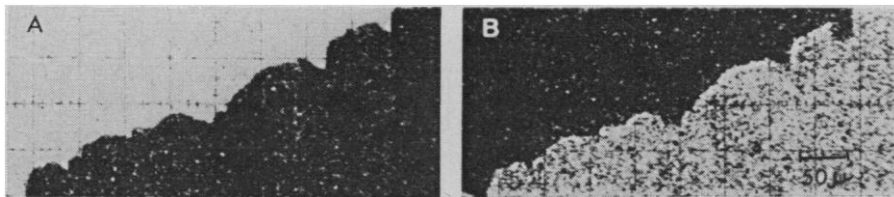


Fig. 3. An aluminum foil 10 μ thick viewed: (A) in transmission and (B) in aluminum K fluorescence.

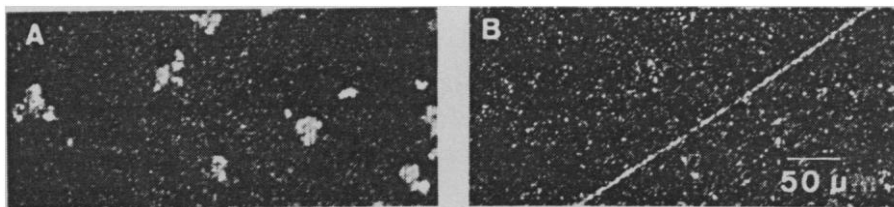


Fig. 4. A sample consisting of sulfur dust and a 2- μ silicon whisker viewed: (A) in sulfur K fluorescence and (B) in silicon K fluorescence.

Element discrimination. A significant fraction (typically 10 to 50 percent) of the energy absorbed from the incident x-ray beam is reemitted as characteristic fluorescent radiation. By selecting pulse heights from the proportional counters which correspond to the characteristic K radiation of a given element or ion, for instance, one can form a micrograph of the distribution of that element. Since the x-ray fluorescent spectra are relatively simple (in contrast to optical spectra), the separation of the characteristic K radiation of one element from the emission lines of other elements is not difficult. A more serious difficulty arises from Thomson scattering of the incident radiation, both from air molecules and from the sample. Although no spectral lines are present, some radiation from this continuum dilutes the desired signal. This effect appears to limit the ultimate sensitivity of the microscope in the detection of small concentrations of a given element in the presence of other more abundant scatterers. The effect of scattering from air molecules has been reduced considerably by the incorporation of a beam stop just behind the sample, as shown in Fig. 1. With the energy resolution of proportional counters it is easy to discriminate between elements of moderate atomic

weight differing in atomic number by 2 or more. An improvement in counter resolution, perhaps by the use of lithium-drifted silicon detectors, would make it possible to discriminate between adjacent elements and would reduce the problem of elastically scattered radiation.

Exposure time and sensitivity. In order to avoid excitation of mechanical resonances of the sample transducer, the fast (x -direction) raster motion of the sample is done at 1 scan per second. Forming a complete picture takes 1 or 2 minutes at this rate, and the counting rates with the 2- μ pinhole are high enough ($\approx 10^4$ per second from a sample of optimum thickness) so that an image of adequate quality is formed in this time. For a pinhole of a different diameter, the necessary exposure time for equivalent image quality is inversely proportional to the square of the resolution size. The limiting sensitivity of the microscope to small concentrations of a particular element can be expressed as a minimum amount of mass per unit area. Calculations indicate that 10^{-6} to 10^{-9} g/cm² should ultimately be detectable at a resolution of 2 μ , although at present this sensitivity has not been reached.

Radiation dosage. A typical exposure

of several minutes with the use of a 2- μ pinhole subjects a thin specimen to a radiation dose of the order of 1000 rad. Although this is usually a fatal dose for mammalian cells, it is not too serious for plant cells or bacteria. It should generally be possible to study living cells with this technique without killing them.

Some results obtained during the initial operation of the microscope are shown in Figs. 2-4. We began by looking at 200 mesh per inch (80 grids per centimeter) copper grid, ordinarily used as a sample substrate for electron microscopy. With the 3.5-keV cutoff of the condensing mirror, only elements lighter than potassium can be examined by fluorescence, and therefore we formed a shadowgram by setting the discriminator to detect elastic scattering from radiation passing through the copper grid. For this purpose the beam stop was removed. This is, of course, an extremely inefficient way to detect the transmitted radiation. The result is shown in Fig. 2, at three different magnifications (easily varied by simply changing the scan amplitude). At the highest magnification the sharpness of the grid contours is consistent with our predicted resolution.

Figure 3 shows two views of a piece of rough-edged aluminum foil 10 μ thick. In Fig. 3A the elastically scattered transmitted beam was detected; in Fig. 3B aluminum K radiation has been selected for viewing.

Figure 4 demonstrates how it is possible to discriminate between different elements. Here some sulfur dust was placed on a thin plastic film, and, in addition, a silicon whisker 2 μ in diameter (of the type used to generate the pinhole) was also placed on the film. Figure 4A shows the result when sulfur K radiation (2.3 keV) is selected, Fig. 4B when silicon K radiation (1.7 keV) is selected. Traces of sulfur are barely visible in Fig. 4B, an indication that there is a slight overlap in the distribution of pulse heights. A micrograph of this same specimen made in *transmission*, as in Fig. 2, showed no discernible structure whatsoever. This result indicates the importance of detecting fluorescent reemission rather than transmission (or absorption) in order to obtain sufficient contrast with thin specimens. The exposure time for all these pictures was roughly 2 minutes.

One can imagine several variations of the present microscope. The technique of selecting pulse heights corresponding to only one element at a time

is wasteful; all detectable chemical species can be photographed at the same time by the use of multiple display oscilloscopes. Alternatively the pulse height information could be recorded for later analysis, perhaps digitally, with the possibility of improving the picture quality through application of image-enhancement techniques.

An interesting possibility is to form a demagnified image of the pinhole, with the use of reflection optics, and scan the sample through the focus. This would provide greater resolution without a loss in counting rate, in contrast to the present inverse-square trade-off.

By operating the synchrotron at higher energy, thicker samples and higher atomic numbers could be examined. The same result can be achieved more efficiently by the installation of a high-field magnetic "undulator" (a magnet with a row of pole pieces for producing a spatially alternating field) in a synchrotron straight section, thus increasing the intensity of the synchrotron radiation and extending its spec-

trum to higher energies. A gain in counting rate, hence improved sensitivity, would also result.

PAUL HOROWITZ

JOHN A. HOWELL

Physics Department, Harvard University, Cambridge, Massachusetts

References and Notes

1. See, for example, J. D. Jackson, *Classical Electrodynamics* (Wiley, New York, 1962), pp. 481-488.
2. P. Kirkpatrick and H. H. Pattee, in *Handbuch der Physik*, S. Flügge, Ed. (Springer-Verlag, Berlin, 1957), p. 305.
3. P. Horowitz and J. A. Howell, in preparation.
4. R. L. Fleischer, P. B. Price, R. M. Walker, *Annu. Rev. Nucl. Sci.* **15**, 1 (1965).
5. W. Desorbo and H. E. Cline, *J. Appl. Phys.* **41**, 2099 (1970).
6. R. S. Wagner and W. C. Ellis, *Trans. Amer. Inst. Min. Metall. Eng.* **233**, 1053 (1965).
7. We are grateful to E. M. Purcell for suggesting the idea for this microscope, and for many inspiring discussions. We also thank R. V. Pound and the CEA staff. We thank R. S. Wagner, Bell Telephone Laboratories, for supplying us with the silicon whisker. This work was supported by grants from the Advanced Research Projects Agency, the National Science Foundation, the Committee on Science Research Support of the Faculty of Arts and Sciences, Harvard University, and the Alfred P. Sloan Foundation. One of the authors (P.H.) is an Alfred P. Sloan Fellow.

15 August 1972

Mercury Detection by Means of Thin Gold Films

Abstract. *The adsorption of elemental mercury vapor on a thin (several hundred angstroms) gold film produces resistance changes in the film. An instrument for the detection of mercury based on this phenomenon is simple and rapid and requires no chemical separations other than passage of the vapor sample through a few standard dry filters. The instrument is portable, and the technique is directly applicable to environmental problems and geochemical prospecting. The limit of detection of the prototype instrument is 0.05 nanogram of mercury.*

In recent years much attention has been devoted to the development of methods for the detection of low concentrations of Hg, both for environmental studies and for geochemical prospecting. A portable instrument capable of rapid, inexpensive analysis is desirable for these purposes. Most semi-portable devices for the detection of low concentrations of Hg have relied on the atomic absorption technique. A variety of modifications have been described, all based on the fact that Hg absorbs at 2537 Å (1, 2). A serious limitation, however, is the presence of interfering substances such as H₂O, O₃, SO₂, and a variety of organic compounds and fine particulates (2). These absorb or scatter electromagnetic energy in the spectral region of interest. As a result of the efforts made to overcome these interferences, the resulting instruments have lost either their portability or their sensitivity, or both.

We have developed an extremely

sensitive and portable Hg detector (3) based on the phenomenon that a thin Au film undergoes a significant increase in resistance upon the adsorption of Hg vapor. This resistance change is linear in nanogram concentrations.

Gold films are prepared by vacuum evaporation on ceramic or glass substrates in a conventional high-vacuum system (10⁻⁶ torr) with the use of a Cr underlayer and no substrate heating. After preparation, the films are an-

nealed in the atmosphere at 150°C. Problems are encountered at higher annealing temperatures (4). The film resistances range from 300 to 1500 ohms. Their thicknesses vary between 400 and 75 Å, with sheet resistivities of 2 to 10 ohms per square, respectively.

A diagram of the instrument is shown in Fig. 1. Two films of equal resistance are used, one as a sensor and the other as a reference. They are contained within a Plexiglas chamber designed to allow a constant flow of carrier gas to pass over the films. The films are connected into opposite arms of a simple d-c bridge circuit and balanced.

The Au films extract Hg from a carrier gas, normally air filtered through activated charcoal. There are two ways that the sample can be introduced into the carrier gas. If the sample is a solid, for example, a biological sample or a soil, it is decomposed and the Hg is concentrated on a noble metal collector. This Hg, in turn, is liberated in the furnace (A in Fig. 1) and then surged into the flow path of the instrument. If the sample is already a vapor, it is injected with a syringe through a rubber septum (B in Fig. 1). This method of introduction can be modified to permit continuous sampling, thereby bypassing the hypodermic introduction.

Before the carrier gas enters the film chamber, the gas is scrubbed of H₂O vapor and acid vapors such as H₂S in a filter train containing MgClO₄ and Ascarite. The airstream is then divided into two fractions. One fraction is scrubbed of Hg by passage over PdCl₂ (5) before it enters the reference chamber. The other fraction is passed over the sensing film. Changes in the resistance of the sensing film are due to Hg adsorption, and variations in the film resistance due to thermal fluctuations or other adsorbing gases are neutralized.

Two factors which affect the sensitivity of the instrument are film thick-

Table 1. Precision data for the Au-film Hg detector; S.D., standard deviation.

Hg vapor standard	Amount of Hg		S.D. (ng)	S.D. (%)	99% tolerance interval (ng)	Determinations (No.)
	Mean (ng)	Range (ng)				
1	0.5	0.47- 0.53	0.03	6	0.09	17
2	1.1	1.05- 1.17	.04	4	.12	16
3	2.2	2.1 - 2.3	.07	3	.21	16
4	3	2.8 - 3.2	.13	4	.39	16
5	11	10.2 -12.0	.62	6	1.9	15
6	25	21.1 -29.2	2.6	10	8.0	15